DOI: 10.1002/anie.201201971

Photoluminescence

Crystal-Plane-Dependent Photoluminescence of Pentacene 1D Wire and 2D Disk Crystals**

*Ji Eun Park, Minhyeok Son, Misun Hong, Gyeongjin Lee, and Hee Cheul Choi**

Photoluminescence (PL) is an important optical phenomenon that has been widely studied for the development of light-based applications, including displays,[1] lasers,[2] sensors,[3] and biotags.[4] Traditionally, PL has been studied for ensemble organic [5] and inorganic compounds in solution,[6] and solid-state inorganic semiconductors that possess direct band-gap energies corresponding to visible-light wavelengths.[7,8] Interest has recently moved to the PL activity of low-dimensional inorganic and organic conducting or semiconducting materials toward developing applications in flexible and cost-effective optical[9–11] and optoelectronic devices.[12,13] PL activity of geometrically well-defined organic molecular and polymeric structures has been of particular interest owing to their recently demonstrated optical-waveguiding[14,15] and lasing properties.[16]

For ensemble organic molecular systems in solution, the local arrangement of molecules in the solvent affects their ability to absorb light [17] as well as their corresponding PL properties, as demonstrated in the case of various H-aggregate and J-aggregate systems.[18,19] Such PL that is dependent on the molecular arrangement, might also be a property of low-dimensional organic structures because many low-dimensional materials frequently have well-defined crystal planes in which unit molecules are arranged in a regular fashion with specific orientations. Therefore, the arrangement of molecules in a particular crystal plane could affect the overall PL process, and ultimately the overall quantum yield of PL.

To examine the influence of crystal planes of low-dimensional organic crystals on their PL properties, it is necessary to have access to a series of crystals of the same crystal structure, but of different crystal geometry. Although the influence of the crystal planes of inorganic crystals on their chemical properties has recently been reported, for example, the face-selective electrostatic adsorption of non-zinc complexes on ZnO nanowires[20] and the surface-dependent photoreactivity of anatase TiO_2 crystals,[21] very little is known about the influence of the crystal planes of organic crystals on their properties, mainly because of the lack of synthetic methods for obtaining homogeneous organic crystals in various geometries.

We have recently reported that highly conjugated molecules can be crystallized into low-dimensional structures with various geometrical shapes, such as *m*-aminobenzoic acid helical nanobelts,[22] C_{60} hexagonal disks,[23] tetra(4-pyridyl)-porphyrin rectangular nanotubes,[24] and copper hexadecafluoro-phthalocyanine ($F_{16}CuPc$) nanoribbons[25] by a physical vapor growth process in a horizontal system;[26] this process is also known as the vaporization–condensation–recrystallization (VCR) process. The VCR process can also be used for the preparation of organic crystals of homogeneous structure in various geometries because the key growth parameters of the process, such as precursor temperature (T_p), substrate temperature (T_s), and flow rate, can be fine tuned. Herein, we report the use of the VCR process for the selective synthesis of pentacene 1D wires and 2D disks, which exhibit an unprecedented crystal-plane-dependent PL activity.

Geometrically well-defined pentacene 1D wires and 2D disks were selectively synthesized using the VCR process at two different precursor temperatures (Figure 1a). Pentacene 1D wires and 2D disks were obtained at $T_p = 350\,^{\circ}C$ and $325\,^{\circ}C$, respectively, on a Si(100) substrate after a reaction time of 15 minutes (Figure 1b and c). Most of the pentacene 1D wires had a rectangular cross-section with an approximate average width of 600 nm and an average thickness of 200 nm. The average length of the 1D wires was approximately 10 μm, although significantly longer wires (over 100 μm) were also observed. The pentacene 2D disks generally had a round shape with an average thickness of approximately 100 nm. The diameter of the disks varied quite widely from 2 to 10 μm. AFM images of a 1D wire and a 2D disk with a thickness of 250 and 100 nm, respectively, are shown in the insets of Figure 1b and c.

The crystal structures of pentacene 1D wires and 2D disks were characterized in detail using X-ray diffraction (XRD; see the Supporting Information, Figure S1) and selected-area electron diffraction (SAED; Figure 1d and e). The SAED and XRD data confirmed that both the pentacene 1D wires and 2D disks are single crystals of high crystallinity: the SAED pattern exhibited well-defined individual electron

[*] J. E. Park, M. Son, M. Hong, G. Lee, H. C. Choi
Department of Chemistry and
Division of Advanced Materials Science
Pohang University of Science and Technology
San 31, Hyoja-Dong, Nam-Gu, Pohang 790-784 (Korea)
E-mail: choihc@postech.edu
Homepage: http://www.postech.ac.kr/chem/nmrl

[**] This work was supported by the National Research Foundation of Korea (NRF) grant funded by MEST (2010-0029649, 2010-0029711, and 2010-00285) and KOSEF through EPB center (2010-001779). This work was supported by the Center for Advanced Soft Electronics under the Global Frontier Research Program of the Ministry of Education, Science and Technology, Korea (2011-0031628). We would like to thank Prof. Taiha Joo at the Department of Chemistry of POSTECH for fruitful discussions. H.C.C. thanks the World Class University (WCU) program (R31-2008-000-10059-0). We are thankful for the use of the 5C2 beamline at Pohang Accelerator Laboratory (PAL) for powder XRD experiments. TEM data were obtained from Korea Basic Science Institute (KBSI).

Supporting information for this article is available on the WWW under http://dx.doi.org/10.1002/anie.201201971.

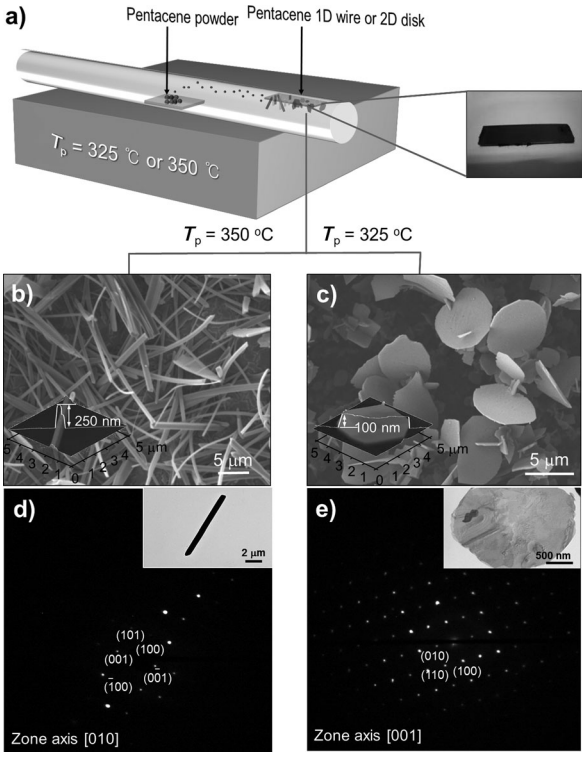

Figure 1. Synthesis and structure of pentacene 1D wires and 2D disks. a) Schematic view of the use of the vaporization–condensation–recrystallization (VCR) process for the synthesis of pentacene 1D wires and 2D disks. b) and c) SEM images of pentacene 1D wires and 2D disks, respectively (scale bar: 5 μm). The insets are AFM images of representative pentacene 1D wires and 2D disks with height profiles. d) and e) Selected-area electron diffraction (SAED) pattern images of pentacene 1D wires and 2D disks depicting zone axes of [010] and [001] for 1D wires and 2D disks, respectively. The insets are the corresponding TEM images (scale bars: d) 2 μm and e) 500 μm).

diffraction spots rather than circular lines, and the XRD pattern exhibited sharp peaks. Both the pentacene 1D wires and 2D disks had triclinic crystal structures. Their powder XRD patterns matched well with that of the previously reported bulk pentacene single crystals grown by the vapor-transport method at 550 K, in that all the patterns showed intense diffraction peaks from the {001} planes.[27] One important feature of the diffraction pattern of the 1D wires is the presence of a (010) peak, a feature, which has not been reported in any other previously reported forms of pentacene. The presence of the (010) plane is critical for the PL, which is only observed in the case of pentacene 1D wires (see below for a detailed explanation). The SAED patterns of pentacene 1D wires and 2D disks confirm that pentacene 1D wires grow along the [100] direction, and that the main planes of pentacene 1D wires and 2D disks are (010) and (001), respectively (Figure 1 d and e).[28]

The T_p value determines whether pentacene 1D wires or 2D disks are formed (see the Supporting Information, Figure S2). Whereas 2D disks were formed at temperatures below 330 °C, 1D wires were dominantly formed at higher temperatures (above 350 °C). The change in crystal morphology occurs in the T_p region between 325 and 350 °C, in which a gradual decrease in 2D disk population with a corresponding increase of the 1D wire population is clearly observed as the temperature rises.

It has been perceived that pentacene, like tetracene and anthracene, crystallizes as film-type 2D structures,[29,30] which is the equilibrium crystal shape (ECS) of pentacene.[31] It is therefore quite remarkable that we have shown that pentacene molecules can crystallize selectively into two distinct geometries, 1D wires and 2D disks, crystal forms that are generated at T_p values that differ by only 25 °C.

To investigate the growth process in more detail, the samples were allowed to grow for various lengths of time (see the Supporting Information, Figure S3). Under the optimized conditions for the growth of pentacene 1D wires ($T_p = 350$ °C and Ar flow rate = 60 sccm), 2D disks were formed at an early stage (< 5 minutes). After longer growth times ($\approx$10 min), 1D wires were found to have grown out of the 2D disks, in a direction normal to the (100) edge planes (see the Supporting Information, Figures S3a and c). After even longer growth times (> 15 minutes), only 1D wires were observed, thus suggesting the 2D disks had been converted into 1D wires. At a T_p value of 325 °C, only 2D disks are formed in all examined growth times (see the Supporting Information, Figure S3b). These observations imply that 1D wires are formed by continuous crystal growth along the [100] direction of 2D disks (i.e., normal to the (100) plane in the ECS of pentacene), a process in which (010) planes are formed parallel to the wire growth axis (see the Supporting Information, Figure S3c). Thus, the successful outgrowth of 1D wires from the (100) plane of pentacene 2D disks indicate that the thermal energy that is equivalent to 350 °C is enough to overcome the surface energy barrier of the (010) plane (6.4 meV Å^{-2}) so that the wires can grow out of the (100) or (001) planes, which have surface energies of 4.8 and 3.1 meV Å^{-2}, respectively.[31]

One remarkable difference between pentacene 1D wires and 2D disks is their PL activity. The absorption spectra of pentacene 1D wires exhibit four well-resolved absorption peaks at 535, 576, 625, and 661 nm (Figure 2 a, black line). The first two peaks (535 and 576 nm) are attributed to the transition between the $S_{0,0}$ state (ground electronic state with $v = 0$) to the $S_{1,1}$ state (first excited electronic state with $v = 0$), and the last two peaks (625 and 661 nm) are attributed to the transition $S_{0,0} \rightarrow S_{1,0}$. There are two peaks for each transition; the doubling originates from the Davydov splitting of the excited vibrational states, a phenomenon that is observed in crystalline structures.[32,33] A similar absorption pattern is observed for the pentacene 2D disks (Figure 2 a, red line), but the overall absorbance is significantly lower than that of the pentacene 1D wires. The PL spectrum of pentacene 1D wires exhibits very strong well-resolved fluorescence peaks ($\lambda_{ex} =$ 355 nm) between 560 and 750 nm (Figure 2 d, black line); the PL of the 2D disks is negligible (Figure 2 d, red line). It should be noted that such an intense and highly resolved PL spectrum has not been reported in the case of pentacene thin films and pentacene crystals. Interestingly, another group of four well-resolved PL peaks appear in the region of 400–500 nm, a feature that is unprecedented and requires further in depth studies. The remarkable difference in the PL proper-

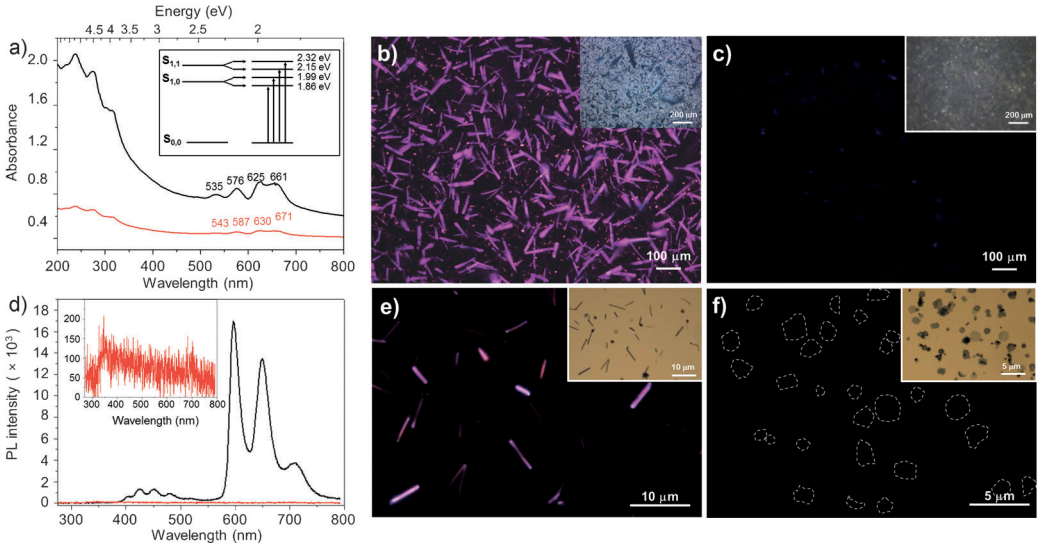

Figure 2. PL activity of pentacene 1D wires and 2D disks. a) Absorption spectra of pentacene 1D wires (black) and 2D disks (red). The inset shows the energy-level diagram for excitonic states of pentacene 1D wires. b) and c) Fluorescence microscope images (low magnification) of as-grown pentacene 1D wires and 2D disks, respectively (scale bar: 100 μm). Insets are the corresponding bright-field optical microscope images (scale bar: 200 μm). d) PL spectra of pentacene 1D wires (black) and 2D disks (red). The inset is an enlarged PL spectrum of pentacene 2D disks. e) and f) PL images of individual pentacene 1D wires and 2D disks, respectively (scale bars: e) 10 μm and f) 5 μm). The corresponding bright-field optical microscope images are shown as insets (scale bars: inset of e) 10 μm and inset of f) 5 μm). The dotted lines in f) indicate the positions of pentacene 2D disks. The excitation wavelength is 330–380 nm, and the irradiation time is 500 ms.

ties between pentacene 1D wires and 2D disks is again apparent in their fluorescence microscope images (λ_{ex} = 330–380 nm and λ_{em} = 420 nm with a long-pass filter). Whereas pentacene 1D wires show intense PL, pentacene 2D disks show almost no PL (Figure 2b and c). The PL images taken from individual pentacene 1D wires (Figure 2e) and 2D disks (Figure 2f) further emphasize the fact that PL activity is only observed in pentacene 1D wires. The parallel contacts of 1D wires and 2D disks on substrates were confirmed by SEM images taken at a tilt angle of 45° (see the Supporting Information, Figure S4).

Considering that the main crystal plane of pentacene 2D disks is (001) and that of the 1D wires is (010), the dramatic difference in PL between 1D wires and 2D disks can be attributed to the alignment of pentacene molecules on each crystal plane relative to the direction of incident light. This phenomenon has been previously demonstrated by the optical absorption and emission processes in self-assembled molecular arrays such as α-sexithiophene[34] and in single crystals of thiophene and phenylene.[35] The key factor that determines the PL activity in these cases is the orientation of the dipole moment of arrayed molecules relative to the direction of the electric-field component of the incident light. That is, if the electric field of incident light is parallel to the dipole moment of arrayed molecules, the transition dipole moment becomes non-zero, and thus PL is maximized with a high absorption cross section.[36] In the case of pentacene 1D wires and 2D disks, pentacene molecules have significantly different arrangements on (010) and (001) planes (Figure 3). A dipole moment along the long axis of pentacene is induced by incident light (Figure 3a).[37] As a result of the way the pentacene molecules are packed (Figure 3b), the induced dipole moment of the array of pentacene molecule in the (010) plane is almost parallel (18°) to the electric field of incident light (Figure 3c). On the other hand, in the (001) plane the induced dipole moment of the arrayed pentacene molecules is almost normal (72°) to the direction of the electric-field component of incident light (Figure 3d). Therefore, the absorption of light in the (010) plane is maximized and should exhibit strong PL. Also, the absorption of light in the (001) plane is weak and should

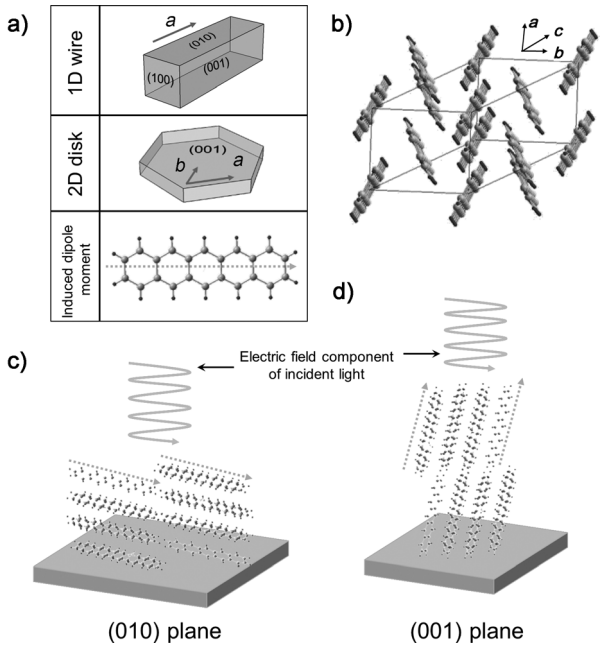

Figure 3. The mechanism for the crystal-plane-dependent PL activity. a) Main crystal planes of pentacene 1D wires and 2D disks, and the induced dipole moment in pentacene. b) Model of the triclinic crystal structure of pentacene. c) Interaction between the dipole moment of pentacene induced in the (010) plane and the electric field of incident light. d) Interaction between the dipole moment of pentacene induced in the (001) plane and the electric field of incident light.

exhibit weak PL. This prediction was confirmed experimentally through the absorption spectra (Figure 2a). We confirmed that an equal number of pentacene molecules contributed to the absorption spectra of the 1D wires and 2D disks by comparing the absorbance of the solutions of dissolved 1D wires and 2D disks to those of solutions of calibrated reference concentrations (see the Supporting Information, Figure S5).

Both pentacene 1D wires and 2D disks have (001) planes, but only the 1D wires have a (010) plane. 1D wires can lie on the substrate in two ways: the 1D wire can lie on the substrate with the (010) plane or the (001) plane parallel to the substrate surface. Therefore, pentacene 1D wires should only exhibit PL when they lie in such a way that the (010) plane is normal to the incident light. To prove this, we performed TEM and SAED experiments correlated with PL imaging: 1D wires were transferred onto a TEM grid by stamping; for each stamped wire, the identity of the crystal plane that was parallel to the grid was determined using SAED; the wires were then imaged using a fluorescence microscope (Figure 4). The data showed that only those 1D wires with (010) planes parallel to the substrate were PL active (Figure 4a–c; PL active wire indicated using a yellow arrow). On the other hand, the 1D wires that were PL inactive were found to lie with their (001) planes parallel to the substrate (4d–f; PL inactive wire indicated using a yellow arrow); this situation is identical to when a 2D disk lies on a substrate (Figure 4g–i).

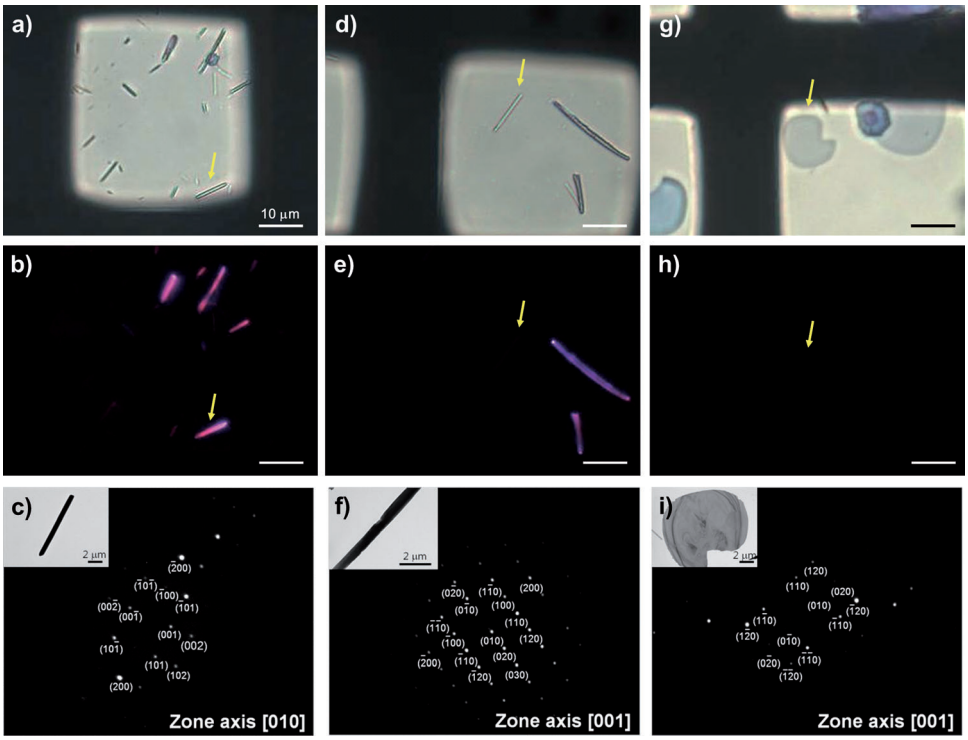

Figure 4. Results of TEM and SAED experiments with correlated PL imaging. a)–c) TEM, PL, and SAED pattern images, respectively, of a pentacene 1D wire in which the (010) plane is parallel to the substrate. d)–f) TEM, PL, and SAED pattern images, respectively, of a pentacene 1D wire in which the (001) plane is parallel to the substrate. g)–i) TEM, PL, and SAED pattern images, respectively, of a pentacene 2D disk in which the (001) plane is parallel to the substrate. The objects indicated by yellow arrows are the examined samples (scale bars: a), b), d), e), g), and h) 10 μm; insets of c), f), and i) 2 μm).

The crystal-plane-dependent PL activity described herein is distinct from recently reported crystallization- or aggregation-induced emission enhancement, such as the enhancement in PL from single crystalline C_{60} disks[23] and C_{70} cubes,[38] or the PL from amorphous hexaphenylsilole aggregates[39] and 1-cyano-*trans*-1,2-bis(4′-methylbiphenyl)ethylene;[40] these examples do not show crystal-plane-dependent PL.

We then examined the effect of crystal-plane-dependent PL activity on the photoresponse of a pentacene 1D wire device. The pentacene 1D wire devices were fabricated by dispersing free-standing pentacene 1D wires on a SiO_2/Si substrate, upon which Au/Cr source and drain electrodes were pre-patterned (Figure 5a). Two different types of devices were fabricated: one having pentacene 1D wires with the (010) plane parallel to the substrate (Figure 5b), and the other one with the (001) parallel to the substrate (Figure 5c). Before measuring the photoresponse, the PL activity associated with each crystal plane was confirmed using a fluorescence microscope (Figure 5b and c, inset images). The PL active 1D wire device exhibited an approximate fourfold increase in photocurrent upon its illumination with UV light ($\lambda_{ex} = 365$ nm) under constant bias voltage ($V_{SD} = 10$ V; Figure 5d); the PL inactive 1D wire device exhibited a negligible change in current upon its illumination with UV light (Figure 5e). This result implies that the photoelectric activity of pentacene crystals is highly dependent on the types of crystal planes that are present in the crystal as well as the alignment of the crystal planes relative to the direction of incident light.

In summary, we have demonstrated the crystal-plane-dependent PL activity of pentacene 1D wires and 2D disks, the crystal structures of which are identical. The pentacene 1D wires and 2D disks were selectively synthesized using the VCR process at different T_p values. The PL activity of pentacene crystals was highly dependent on its geometry, which determines the specific crystal plane that interacts with the incident light. Pentacene 1D wires that possessed (010) and (001) planes exhibit strong PL when the light beam is normal to the (010) plane. On the other hand, no PL is detected when the light beam is normal to the (001) planes of both pentacene 1D wires and 2D disks. The crystal-plane-

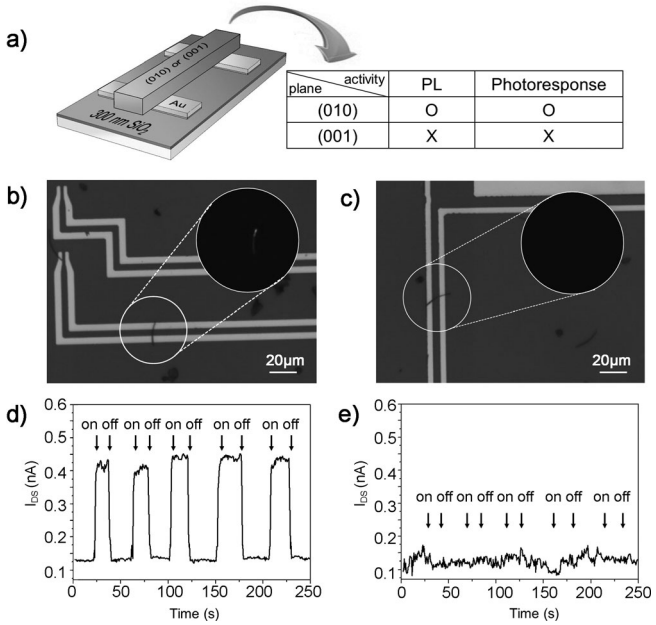

Figure 5. Crystal-plane-dependent photoresponse of pentacene 1D wire. a) Schematic view of a pentacene 1D wire device. The table summarizes the data related to the PL and photoresponse activities of the device. b) and c) Optical microscope images of pentacene 1D wire devices in which the 1D wire lies with the (010) plane and the (001) plane parallel to the substrate, respectively. Inset PL images show the pentacene 1D wire of b) is only PL active. d) and e) Photoresponses from devices in b) and c), respectively, upon their illumination with UV light ($\lambda_{ex} = 365$ nm). The applied bias voltage (V_{DS}) is 10 V without applying gate voltage.

dependent PL is attributed to the arrangement of pentacene molecules in the (010) and (001) planes; the level of absorption of incident light is determined by the orientation of the direction of the electric field of the incident light relative to the direction of the dipole moment of pentacene that is induced within each plane. It was also demonstrated that such a crystal-plane-dependent PL activity strongly affects the optoelectronic performance of pentacene-based devices; pentacene 1D wire devices showed a strong photoresponse when the (010) crystal plane was normal to the beam of incident light.

Experimental Section

Synthesis of pentacene 1D wires and 2D disks: Pentacene powder (5 mg, 99.9%, purchased from Sigma Aldrich and used without further purification) and a small piece of silicon wafer were placed in the middle and at the end of a quartz tube, respectively. The quartz tube was then placed into a horizontal heating-tube furnace, in such a way that the pentacene powder was located at the center of the heating furnace (Figure 1a). After flushing the tube with Ar gas (99.999%) for 10 min, the quartz tube was heated from room temperature to the designated precursor temperature (T_p), 350 °C for the 1D wire or 325 °C for the 2D disk, under an atmosphere of Ar; once the designated precursor temperature (T_p) was reached, the system was allowed to remain at that temperature for 15 min. For the growth mechanism studies, the growth was allowed to take place for various lengths of time (1, 5, 10, 15, and 20 min) and at various precursor temperatures (between 300 and 400 °C with intervals of 25 °C, and between 325 and 350 °C with intervals of 5 °C).

Structure characterization: The morphology of pentacene crystals, their growth direction, and their zone axes were characterized by scanning electron microscopy (SEM, JEOL, JSM-7410F) and transmission electron microscopy (TEM, Carl Zeiss, EM 912 omega). X-ray diffraction data were obtained from the 5C2 beamline at Pohang Accelerator Laboratory (PAL).

Photoluminescence spectroscopy and imaging: The sample was excited using a laser (Crystal GmbH, 355 nm) and the resultant fluorescence signal was collected by a parabolic mirror, dispersed by a monochromator (Acton research, spectrapro300i), and detected with a charge-coupled device detector (Roper scientific, RTE/CCD-128-HB), equipped with a 395 nm long-pass filter. The PL images of as-grown pentacene 1D wire and 2D disk were obtained using a fluorescence microscope (Olympus microscope) equipped with a fluorescence filter ($\lambda_{ex} = 330$–380 nm, $\lambda_{em} = 420$ nm long pass filter). For the PL imaging of individual 1D wires and 2D disks, the as-grown samples were transferred onto a quartz substrate. The irradiation time for imaging was 500 ms.

Determination of optical absorptivity: UV/Vis absorption spectra were obtained using a UV/Vis spectrometer (Agilent 8453 spectrophotometer). The relative amounts of as-grown 1D wires and 2D disks used for the PL studies were determined by measuring and comparing the optical absorbance ($\lambda = 583$ nm) of both samples after dissolving them in 1,2,4-trichlorobenzene (99+%, Sigma Aldrich).

Fabrication of pentacene 1D wire devices: The devices were fabricated using a standard photolithography technique. Source and drain electrodes were first patterned on SiO_2/Si substrates by depositing 20 nm of thermally evaporated Au over 5 nm of Cr, onto which as-grown pentacene 1D wires were transferred. To evaluate the crystal plane dependence of the photoresponse, devices in which the pentacene 1D wires had their (010) plane parallel to the substrate and devices in which the pentacene 1D wires had their (001) plane parallel to the substrate were selected. The photoresponse was measured by monitoring the current changes, using a semiconductor analyzer (KEITHLEY 4200), upon UV irradiation ($\lambda_{ex} = 365$ nm, ENF-240C/FE). The applied bias voltage between the source and drain electrode (V_{SD}) was 10 V.

Received: March 13, 2012
Published online: May 29, 2012

Keywords: crystal engineering · luminescence · pentacenes · photoluminescence · solid-state structures

[1] G. M. Farinola, R. Ragni, *Chem. Soc. Rev.* **2011**, *40*, 3467–3482.
[2] R. Yan, D. Gargas, P. Yang, *Nat. Photonics* **2009**, *3*, 569–576.
[3] M. J. Sailor, E. C. Wu, *Adv. Funct. Mater.* **2009**, *19*, 3195–3208.
[4] K. Kikuchi, *Chem. Soc. Rev.* **2010**, *39*, 2048–2053.
[5] Y. S. Zhao, H. Fu, A. Peng, Y. Ma, D. Xiao, J. Yao, *Adv. Mater.* **2008**, *20*, 2859–2876.
[6] K. M. C. Wong, V. W. W. Yam, *Acc. Chem. Res.* **2011**, *44*, 424–434.
[7] T. Shimizu-Iwayama, S. Nakao, K. Saitoh, *Appl. Phys. Lett.* **1994**, *65*, 1814–1816.
[8] R. W. Miles, G. Zoppi, I. Forbes, *Mater. Today* **2007**, *10*, 20–27.
[9] M. Law, D. J. Sirbuly, J. C. Johnson, J. Goldberger, R. J. Saykally, P. Yang, *Science* **2004**, *305*, 1269–1273.
[10] Y. S. Zhao, H. Fu, A. Peng, Y. Ma, Q. Liao, J. Yao, *Acc. Chem. Res.* **2010**, *43*, 409–418.
[11] I. L. Medintz, H. T. Uyeda, E. R. Goldman, H. Mattoussi, *Nat. Mater.* **2005**, *4*, 435–446.
[12] Y. Shirota, *J. Mater. Chem.* **2000**, *10*, 1–25.
[13] D. A. Gaul, Jr., W. S. Rees, *Adv. Mater.* **2000**, *12*, 935–946.

[14] K. Takazawa, Y. Kitahama, Y. Kimura, G. Kido, *Nano. Lett.* **2005**, *5*, 1293 – 1296.
[15] Y. S. Zhao, A. Peng, H. Fu, Y. Ma, J. Yao, *Adv. Mater.* **2008**, *20*, 1661 – 1665.
[16] D. O'Carroll, I. Lieberwirth, G. Redmond, *Nat. Nanotechnol.* **2007**, *2*, 180 – 184.
[17] H. Y. Woo, B. Liu, B. Kohler, D. Korystov, A. Mikhailovsky, G. C. Bazan, *J. Am. Chem. Soc.* **2005**, *127*, 14721 – 14729.
[18] E. Da Como, M. A. Loi, M. Murgia, R. Zamboni, M. Muccini, *J. Am. Chem. Soc.* **2006**, *128*, 4277 – 4281.
[19] S. Gadde,, E. K. Batchelor, J. P. Weiss, Y. Ling, A. E. Kaifer, *J. Am. Chem. Soc.* **2008**, *130*, 17114 – 17119.
[20] J. Joo, B. Y. Chow, M. Prakash, E. S. Boyden, J. M. Jacobson, *Nat. Mater.* **2011**, *10*, 596 – 601.
[21] J. Pan, G. Liu, G. Q. Lu, H. Cheng, *Angew. Chem.* **2011**, *123*, 2181 – 2185; *Angew. Chem. Int. Ed.* **2011**, *50*, 2133 – 2137.
[22] S. M. Yoon, I. C. Hwang, N. Shin, D. Ahn, S. J. Lee, J. Y. Lee, H. C. Choi, *Langmuir* **2007**, *23*, 11875 – 11882.
[23] H. S. Shin, S. M. Yoon, Q. Tang, B. Chon, T. Joo, H. C. Choi, *Angew. Chem.* **2008**, *120*, 705 – 708; *Angew. Chem. Int. Ed.* **2008**, *47*, 693 – 696.
[24] S. M. Yoon, I. C. Hwang, K. S. Kim, H. C. Choi, *Angew. Chem.* **2009**, *121*, 2544 – 2547; *Angew. Chem. Int. Ed.* **2009**, *48*, 2506 – 2509.
[25] S. M. Yoon, H. J. Song, I. C. Hwang, K. S. Kim, H. C. Choi, *Chem. Commun.* **2010**, *46*, 231 – 233.
[26] R. A. Laudise, Ch. Kloc, P. G. Simpkins, T. Siegrist, *J. Cryst. Growth* **1998**, *187*, 449 – 454.
[27] C. C. Mattheus, A. B. Dros, J. Baas, A. Meetsma, J. L. de Boer, T. T. M. Palstra, *Acta Crystallogr. Sect. C* **2001**, *57*, 939 – 941.
[28] Because the pentacene 1D wires and 2D disks are triclinic structures, the SAED patterns were obtained by manually tilting the sample stage by about 5 degrees (for (010)) and 10 degrees (for (001)) so that the electron beam was aligned with the internal zone axis.
[29] R. W. I. de Boer, M. E. Gershenson, A. F. Morpurgo, V. Podzorov, *Phys. Status Solidi A* **2004**, *201*, 1302 – 1331.
[30] S. Verlaak, S. Steudel, P. Heremans, D. Janssen, M. S. Deleuze, *Phys. Rev. B* **2003**, *68*, 195409.
[31] J. E. Nothrup, M. L. Tiago, S. G. Louie, *Phys. Rev. B* **2002**, *66*, 121404.
[32] A. S. Davydov, *Theory of Molecular Excitons*, Plenum, Boca Raton, **1971**.
[33] Q. Miao, T.-Q. Nguyen, T. Someya, G. B. Blanchet, C. Nuckolls, *J. Am. Chem. Soc.* **2003**, *125*, 10284 – 10287.
[34] M. A. Loi, E. D. Como, F. Dinelli, M. Murgia, R. Zamboni, F. Biscarini, M. Muccini, *Nat. Mater.* **2005**, *4*, 81 – 85.
[35] S. Hotta, T. Yamao, *J. Mater. Chem.* **2011**, *21*, 1295 – 1304.
[36] D. A. McQuarrier, J. D. Simon, *Physical Chemistry*, University Science Books, California, **1997**.
[37] R. Firouzi, M. Zahedi, *J. Mol. Struct. (Theochem)* **2008**, *862*, 7 – 15.
[38] C. Park, E. Yoon, M. Kawano, T. Joo, H. C. Choi, *Angew. Chem.* **2010**, *122*, 9864 – 9869; *Angew. Chem. Int. Ed.* **2010**, *49*, 9670 – 9675.
[39] Y. Hong, J. W. Y. Lam, B. Z. Tang, *Chem. Commun.* **2009**, 4332 – 4353.
[40] B. K. An, S. K. Kwon, S. D. Jung, S. Y. Park, *J. Am. Chem. Soc.* **2002**, *124*, 14410 – 14415.

